Science of the Total Environment 409 (2011) 3909–3918

Contents lists available at ScienceDirect

Science of the Total Environment

journal homepage: www.elsevier.com/locate/scitotenv

# An examination of groundwater discharge and the associated nutrient fluxes into the estuaries of eastern Hainan Island, China using $^{226}Ra$

Ni Su [a], Jinzhou Du [a,*], Willard S. Moore [b], Sumei Liu [c], Jing Zhang [a]

[a] State Key Laboratory of Estuarine and Coastal Research, East China Normal University, Shanghai 200062, China
[b] Department of Earth and Ocean Sciences, University of South Carolina, Columbia, SC 29208, USA
[c] Key Laboratory of Marine Chemistry Theory and Technology, Ministry of Education, Ocean University of China, Qingdao 266100, China

ARTICLE INFO

*Article history:*
Received 3 February 2011
Received in revised form 7 June 2011
Accepted 8 June 2011
Available online 29 June 2011

*Keywords:*
Radium isotope
Groundwater discharge
Nutrient fluxes
Bay/estuary

ABSTRACT

The nutrient concentrations and stoichiometry in a coastal bay/estuary are strongly influenced by the direct riverine discharge and the submarine groundwater discharge (SGD). To estimate the fluxes of submarine groundwater discharge into the Bamen Bay (BB) and the Wanquan River Estuary (WQ) of eastern Hainan Island, China, the naturally occurring radium isotope ($^{226}Ra$) was measured in water samples collected in the bay/estuary in August 2007 and 2008. Based on the distribution of $^{226}Ra$ in the surface water, a 3-end-member mixing model was used to estimate the relative contributions of the sources to these systems. Flushing times of $3.9 \pm 2.7$ and $12.9 \pm 9.3$ days were estimated for the BB and WQ, respectively, to calculate the radium fluxes for each system. Based on the radium fluxes from groundwater discharge and the Ra isotopic compositions in the groundwater samples, the estimated SGD fluxes were $3.4 \pm 5.0$ $m^3$ $s^{-1}$ in the BB and $0.08 \pm 0.08$ $m^3$ $s^{-1}$ in the WQ, or 16% and 0.06%, respectively, of the local river discharge. Using this information, the nutrient fluxes from the submarine groundwater discharge seeping into the BB and WQ regions were estimated. In comparison with the nutrient fluxes from the local rivers, the SGD-derived nutrient fluxes played a vital role in controlling the nutrient budgets and stoichiometry in the study area, especially in the BB.

© 2011 Elsevier B.V. All rights reserved.

## 1. Introduction

In the coastal zone, there are several pathways for the transport of terrestrial substances from land to sea. One of them, submarine groundwater discharge (SGD), is historically overlooked in the development of near-shore nutrient and water budgets. The SGD is the flow of water through continental margins from the seabed to the coastal ocean along of meters to kilometers, regardless of the fluid composition or the driving force (Burnett et al., 2003; Moore, 2010). However, such water flow is largely unseen and difficult to quantify because it occurs as submarine seeps with patchy, diffuse patterns, which are both spatially and temporally variable, and because most of the water flow occurs at slow rates of discharge (Moore, 1999; Burnett et al., 2006; Dulaiova et al., 2006).

Numerous studies have used direct and indirect measurements to estimate SGD. Lee (1977) used a seepage meter for the direct measurement of SGD. However, a real limitation of any seepage meter is that the small footprint of the instrument can provide only site-specific information (Swarzenski, 2007); a large-scale study requires many deployments that are time consuming and inefficient (Michael et al., 2003). Recently, many studies have developed and utilized geochemical tracers, such as the U/Th decay series (Rn and Ra isotopes), to quantify the SGD rates indirectly (Moore, 1996; Charette et al., 2001; Burnett and Dulaiova, 2003; Swarzenski et al., 2007). These studies build on the differences between the half-life of Ra and Rn and their thorium parents, and the observation that Ra and Rn are usually significantly enriched in the discharging groundwater relative to the coastal surface water; these radiotracers are chemically conservative in the coastal zone. In contrast to seepage meters, the naturally occurring tracers provide local to regional-scale information about groundwater inputs into the coastal ocean.

Recent research has highlighted the significance of SGD as one of the most important vectors for the transport of material to coastal waters (Burnett et al., 1990, 2001, 2002, 2003, 2006; Moore, 1996; Charette et al., 2001; Swarzenski et al., 2001, 2007). SGD often carries elevated concentrations of nutrients, trace elements, radionuclides, and organics due to the biological and chemical reactions at the interface between the freshwater in the aquifer and the salt-water front. These fluxes have the potential to impact the chemical budgets of surface water ecosystems (Moore et al., 2006; Swarzenski, 2007). Even small SGD fluxes may result in large nutrient and trace metal fluxes into the coastal region and lead to changes in water quality by unbalancing stoichiometry, increasing heavy metal concentrations, and stimulating phytoplankton blooms (Krest et al., 2000; Moore et al., 2002). Paytan et al. (2005) demonstrated that groundwater discharge

* Corresponding author. Tel.: +86 21 62232761; fax: +86 21 62546441.
*E-mail address:* jzdu@sklec.ecnu.edu.cn (J. Du).

0048-9697/$ – see front matter © 2011 Elsevier B.V. All rights reserved.
doi:10.1016/j.scitotenv.2011.06.017

could be an important source of nutrients for coral reefs; however, excessive nutrient inputs can negatively impact their survival.

Along the northeastern coastline of Hainan Island, China, there are well-protected ecosystems such as coral reefs, mangroves, and sea grass beds. However, these ecosystems have recently been facing disturbances from human activities, such as increasing agriculture and expanding tourism, as Hainan Island has become a major tourist destination. In addition to current concern about the material carried by rivers into the coastal zone, coastal environmental management should also investigate the groundwater discharge, which can discharge materials into the nearshore marine environment. In some cases, these discharges provide essential nutrients, whereas in other cases, these discharges may upset nutrient balances and contribute toxic materials (e.g., Valiela et al., 1990; Krest et al., 2000; Liu et al., 2001). Our objective in this study was to estimate the submarine groundwater discharge rates into the Bamen Bay (BB) and the Wanquan River Estuary (WQ) of eastern Hainan Island using $^{226}$Ra as tracer. We also evaluated the nutrient fluxes through SGD and their impact on the coastal ecosystem. We expect these studies to provide a baseline against which future changes can be compared.

## 2. Sampling and methods

### 2.1. Study area

Hainan Island is located in the southern part of China, with a coastline length of 1550 km. The climate is classified as tropical monsoon and tropical ocean, with offshore winds prevailing during the winter monsoon season and landward winds prevailing during the summer monsoon season. Each year, tropical storms and typhoons frequently strike the island in August and September, bringing large amounts of rainfall (Mao et al., 2006). Our study focused on the eastern estuaries of Hainan Island, north of the South China Sea (Fig. 1). This area includes three major river systems (the Wenchang, Wenjiao, and Wanquan rivers), and three major ecosystems (coral reef, mangrove, and sea grass beds).

The Wanquan River is the third largest river on Hainan Island, with a total length of ca. 160 km and a drainage area of ca. $3.68\times10^3$ km$^2$. It passes through the third largest city, Qionghai, and flows into the South China Sea via the Wanquan River Estuary on the eastern coast of Hainan Island. The Wanquan River is the most important source of water for the industrial and agricultural production in the city of Qionghai. More than 80% of the local water supply is from surface water and thus is likely to be affected by the discharge of the Wanquan River. Due to the monsoon seasons in this area, ~ 80% of the annual precipitation falls between May and November (Ge et al., 2003). The average annual discharge of the river is 164 m$^3$ s$^{-1}$. During the sampling period, the discharge was 136 m$^3$ s$^{-1}$. The study area is geomorphologically characterized by sand spits, sand bars and islands, which divide the river flow into two branches (north and south). The distribution of sampling locations within the study area was restricted to the lower reaches of the WQ, with a surface area of ca. 1.5 km$^2$ and an average water depth of 2.5 m (Wang et al., 2006).

The Wenjiao and Wenchang rivers flow directly into the Bamen Bay from the east and west parts of the bay, with lengths of 56.0 km and 37.1 km and discharges of 11.6 m$^3$ s$^{-1}$ and 9.09 m$^3$ s$^{-1}$ (total discharge of 20.7 m$^3$ s$^{-1}$), respectively (Zeng and Zeng, 1989; Wang et al., 2006). The Bamen Bay is a typical semi-enclosed water body with a historic surface area of 40 km$^2$, which is now reduced to ca. 20 km$^2$. It connects with the South China Sea through the Qinglan tidal inlet (ca. 9.0 km long). The tidal current here is characterized by an irregular semidiurnal tide, with a diurnal tide for 15 to 18 days followed by a semidiurnal tide for approximately 11 days (Wang, 2002). The Bamen Bay is a shallow water body with an average water depth of 1.0 m in the center part of the bay and 2 to 3 m in the southwestern part of the bay and in the Qinglan tidal inlet (Wang et al., 2006).

Along the east coast of Hainan Island, the surficial aquifer, which has the most interaction with the bay/estuary, is a 3 to 12 m thick unconfined aquifer consisting predominately of silt–sand-gravel. This is typical of the coastal plain deposits throughout much of the eastern Hainan coastal area (Ding et al., 2007). The primary source of groundwater recharge for this aquifer comes from local precipitation (annual precipitation is 187 cm year$^{-1}$) infiltrating the surface sands, with an infiltration coefficient of 0.3 to 0.6 m day$^{-1}$.

### 2.2. Methods

#### 2.2.1. Water samples

Most of the groundwater and bay/estuary water samples in the Bamen Bay and Wanquan River estuary were collected in August 13–27, 2007, and a few groundwater samples were taken in August 2008 (Table 1). The surface water samples (ca. 20 L) in the bay/estuary were collected using a submerged pump at a depth of 0.5 m below the surface. After collection, the samples were filtered immediately through cellulose filters (pore size: 0.45 μm). The filtered water was stored in pre-cleaned polyethylene containers, the entire sample was acidified by HCl to a pH of 2, and a yield tracer of $^{225}$Ra in equilibrium with its parent $^{229}$Th (Eckert & Ziegler Isotope Products, 7229) was added. The samples were thoroughly mixed and then allowed to stand for ca. 6 h to allow equilibration. Next, $NH_4OH$, $KMnO_4$ (0.2 M) and $MnCl_2$ (0.5 M) solutions were added, causing $MnO_2$ to precipitate at a pH of 9; the precipitate was separated from the supernatant and redissolved in $HNO_3$ and $H_2O_2$ (Zhang, 2007). Here, we assume that the quantities of radium and thorium that were recovered from the sample were equal, as much of the original $^{225}$Ra decayed before the further steps were completed. The activity of $^{226}$Ra was determined using alpha spectrometry following the radiochemical separation (Hancock and Martin, 1991). Briefly, a $Pb(NO_3)_2$ solution was added to the acidic solution described above, and Pb(Ra)$SO_4$ was co-precipitated by adding concentrated $H_2SO_4$ and solid $K_2SO_4$. The co-precipitate was centrifuged and redissolved in ethylene diamine tetraacetic acid (EDTA). This solution was passed through an anion exchange column (DOWEX 1X8-200, 100–200 mesh, chloride form, 50 mm height, 7 mm i.d.) and a cation exchange column (DOWEX 50WX8-200, 200–400 mesh, 80 mm height, 7 mm i.d.). Finally, Ra was electrodeposited onto a stainless-steel disk and determined by α-particle spectrometry (Model: Canberra 7200–08).

The groundwater samples (ca. 200 L) were pumped from the wells, then directly pumped through a 0.5 μm polypropylene cartridge pre-filter to remove suspended particles, and then pumped through two $MnO_2$ impregnated cartridges, connected in a series to concentrate radium and to calculate the extraction efficiency (Baskaran et al., 1993). The $MnO_2$-fibers were removed from the cartridge and washed in distilled water to remove salts, then dried and ashed at 550 °C for more than 6 h in a muffle furnace. After cooling, the ashes were weighed and transferred into plastic vials, which were sealed for the determination of $^{226}$Ra and $^{228}$Ra concentrations using a gamma-ray spectrometer (Model: Canberra BE3830). Because $^{226}$Ra concentration is determined using a daughter of $^{222}$Rn, the samples must be stored for at least 20 days for equilibrium concentrations be reached among $^{226}$Ra, its volatile daughter $^{222}$Rn ($T_{1/2}=3.8$ days), and the Rn daughter nuclides (Rutgers van der Loeff and Moore, 1999). The mean extraction efficiency in this study was ~83% rather than the expected >97% observed by Moore (1976). The chemical procedure that we used to make the Mn-fibers is different from that reported by Moore (1976). The fibers we used are polypropylene fibers, not acrylic fibers, and the cooking time in the $KMnO_4$ solution was longer than that reported by Moore (1976). If the cooking time is too long, the Mn-fibers become brittle and break easily, causing the $MnO_2$ to be lost from the fibers and thus reducing the Ra recovery.

The sediment samples were collected using a Van Veen grab sampler in the BB in July 2008. In the laboratory, the samples were

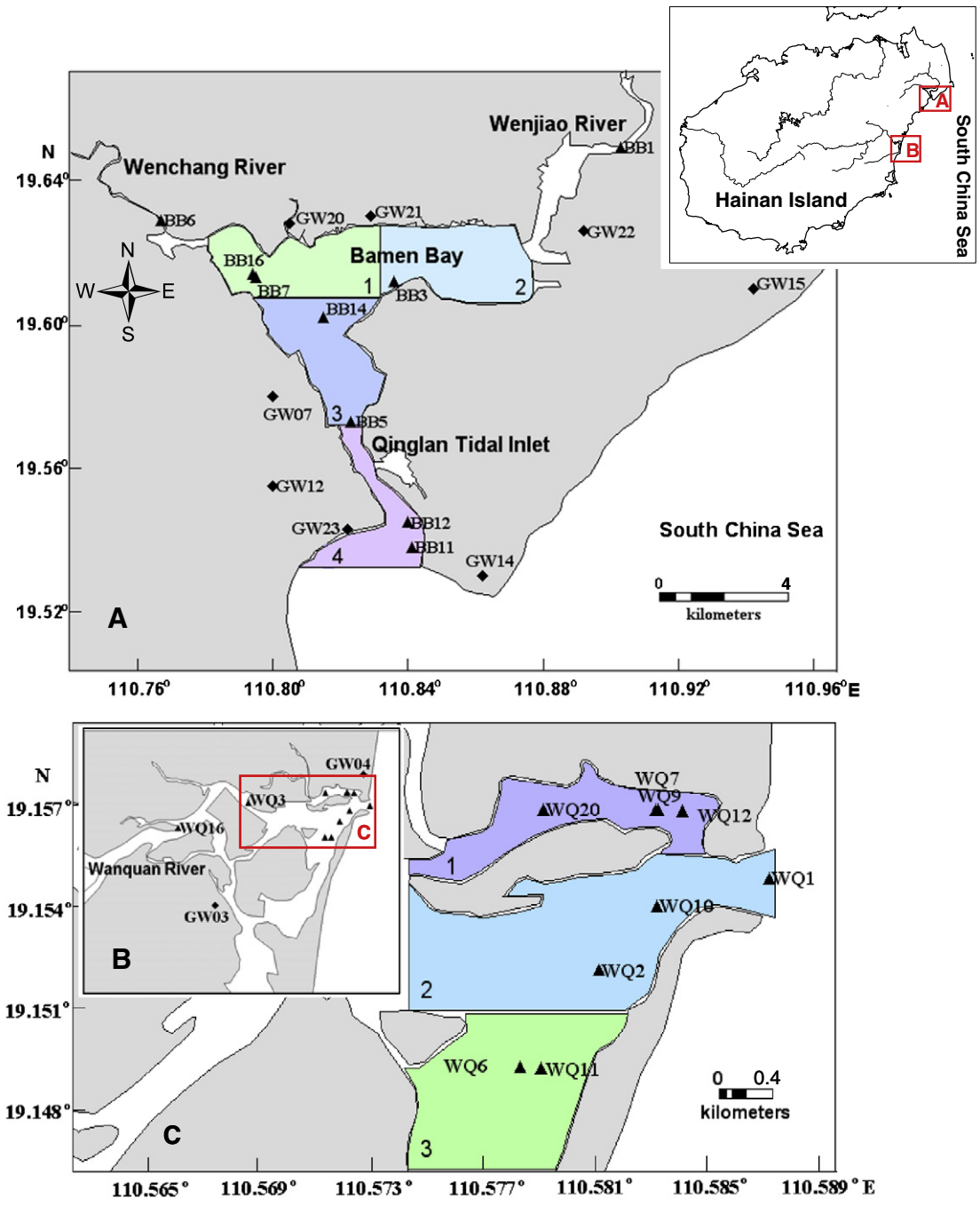


**Fig. 1.** Location maps of the study area. Map A and B: the station locations for the surface water and groundwater samples in the Bamen Bay and Wanquan River estuary regions, respectively. Map C is an expanded view for Map B near the mouth. The BB and WQ regions are divided into four and three boxes. Note stations WQ7 and WQ9 overlap, WQ23 is at the upper reaches of the Wanquan River, and GW10 is in the south of the estuary and not shown in B and C.

dried, weighed, sealed for 3 weeks and measured for $^{226}Ra$ using γ-spectrometry (Model: Canberra BE3830). During the same period, fresh river water samples from BB and WQ (ca. 200 L) were filtered through a series of 0.5 μm polypropylene cartridges to collect suspended particles to estimate the Ra activity in the suspended particulate matter (SPM) (Baskaran et al., 1993). In the laboratory, the polypropylene cartridges were treated similarly to the $MnO_2$-fibers, which were dried, ashed, sealed and measured by γ-spectrometry for $^{226}Ra$ activity.

*2.2.2. Nutrients*

The samples used to measure inorganic nutrient levels were collected at the same stations as the groundwater radium samples. After water collection, the samples were immediately filtered through pre-cleaned 0.45 μm-pore cellulose acetate filters, and the filtrates were poisoned with saturated $HgCl_2$. The nutrient concentrations [$NO_2^-$, $NO_3^-$, $NH_4^+$, $PO_4^{3-}$ and $Si(OH)_4$] were quantified using an autoanalyzer (Model: Skalar SAN$^{plus}$) (Liu et al., 2005). The analytical precision of $NO_2^-$, $NO_3^-$, $NH_4^+$, $PO_4^{3-}$, and $Si(OH)_4$ were 0.01, 0.06, 0.09,

**Table 1**
Surface water sampling stations and activities of $^{226}$Ra (dpm 100 L$^{-1}$) in the Bamen Bay (BB) and Wanquan River estuary (WQ) collected in August 2007.

| Sample | Longitude (°E) | Latitude (°N) | Location | Date (mm/dd/yy) | Water depth (m) | Salinity | $^{226}$Ra | Error | Box |
|---|---|---|---|---|---|---|---|---|---|
| Bamen Bay | | | | | | | | | |
| BB3 | 110.836 | 19.612 | BB | 08/15/2007 | 2.0 | 17.9 | 25.94 | 0.82 | 2 |
| BB5 | 110.823 | 19.573 | BB | 08/15/2007 | 6.0 | 22.6 | 23.66 | 0.72 | 3 |
| BB7 | 110.795 | 19.613 | BB | 08/16/2007 | 4.0 | 9.5 | 33.60 | 1.51 | 1 |
| BB11 | 110.841 | 19.538 | BB | 08/16/2007 | 6.0 | 28.5 | 18.34 | 0.69 | 4 |
| BB14 | 110.815 | 19.602 | BB | 08/25/2007 | 2.0 | 27.4 | 20.38 | 0.60 | 3 |
| BB16 | 110.794 | 19.614 | BB | 08/25/2007 | 2.0 | 8.9 | 34.32 | 0.99 | 1 |
| BB12 | 110.840 | 19.545 | BB | 08/25/2007 | 6.0 | 33.3 | 12.98 | 0.44 | 4 |
| BB1 | 110.903 | 19.648 | Wenjiao River | 08/15/2007 | – | 0.0 | 23.99 | 0.84 | |
| BB6 | 110.767 | 19.629 | Wenchang River | 08/16/2007 | 2.0 | 0.0 | 23.92 | 0.92 | |
| Area-weighted average | | | | | | | 25.40 | 0.37 | 1, 2, 3, and 4 |
| Wanquan River estuary | | | | | | | | | |
| WQ1 | 110.587 | 19.156 | WQ | 08/13/2007 | 3.0 | 33.9 | 12.79 | 0.42 | 2 |
| WQ2 | 110.581 | 19.153 | WQ | 08/13/2007 | 5.0 | 2.4 | 15.30 | 0.52 | 2 |
| WQ6 | 110.578 | 19.150 | WQ | 08/13/2007 | 1.4 | 7.0 | 18.93 | 0.57 | 3 |
| WQ7 | 110.583 | 19.157 | WQ | 08/13/2007 | 1.9 | 4.6 | 17.36 | 0.60 | 1 |
| WQ9 | 110.583 | 19.157 | WQ | 08/14/2007 | 2.7 | 26.6 | 12.12 | 0.47 | 1 |
| WQ10 | 110.583 | 19.155 | WQ | 08/14/2007 | 3.2 | 12.2 | 15.37 | 0.56 | 2 |
| WQ11 | 110.579 | 19.150 | WQ | 08/14/2007 | 1.2 | 6.2 | 17.84 | 0.59 | 3 |
| WQ12 | 110.584 | 19.157 | WQ | 08/26/2007 | 3.0 | 8.7 | 12.36 | 0.62 | 1 |
| WQ20 | 110.579 | 19.157 | WQ | 08/26/2007 | 3.5 | 15 | 12.63 | 0.69 | 1 |
| WQ3 | 110.563 | 19.156 | Wanquan River | 08/13/2007 | 1.4 | 0.0 | 13.57 | 0.58 | |
| WQ16 | 110.549 | 19.151 | Wanquan River | 08/26/2007 | 1.3 | 0.0 | 7.74 | 0.50 | |
| WQ23 | 110.438 | 19.252 | Wanquan River | 08/14/2007 | – | 0.0 | 10.20 | 0.57 | |
| Area-weighted average | | | | | | | 15.60 | 0.20 | 1, 2, and 3 |
| Offshore seawater (average) | | | | 08/20/2007 | | 35.6 | 10.30 | 0.54 | |

0.03 and 0.15 μM, respectively (Liu et al., 2009). The concentration of dissolved inorganic nitrogen (DIN) is the sum of $NO_3^-$, $NO_2^-$ and $NH_4^+$.

## 3. Results

### 3.1. $^{226}$Ra activities in the Bamen Bay and the Wanquan River estuary

The dissolved $^{226}$Ra measurements in the surface water of the BB and WQ are shown in Table 1. The $^{226}$Ra activities in the BB ranged between 13.0 and 34.3 dpm 100 L$^{-1}$, within a salinity range of 0–33.3. The maximum activity, 34.3 dpm 100 L$^{-1}$, was found at a salinity of 8.9. In the WQ, the $^{226}$Ra activities ranged from 7.7 to 18.9 dpm 100 L$^{-1}$, with the maximum activity of 18.9 dpm 100 L$^{-1}$ observed at a salinity of 7.0. The relationship between the dissolved $^{226}$Ra and salinity showed a pronounced enrichment of Ra (excess Ra) in the BB and WQ relative to the theoretical conservative mixing between the river and ocean end-members (Fig. 2). Early investigations concluded that the origin of this excess Ra was the desorption of Ra from river-borne suspended particles and diffusion from the bottom sediments (Li et al., 1977; Elsinger and Moore, 1980; Moore, 1981; Key et al., 1985). However, more recent studies have concluded that excess Ra from coastal groundwater is another important source in some estuaries (Miller et al., 1990; Hussain et al., 1999; Krest et al., 1999; Moore, 1999; Yang et al., 2002).

Because samples are not homogeneously distributed within a bay/estuary, the area-weighed average radium activities ($Ra_{avg}$) were calculated as outlined by Garcia-Solsona et al. (2010).

$$Ra_{avg} = \frac{\sum_{i=1}^{n} \left( Ra^{i}_{avg} \cdot A_i \right)}{A_{tot}} \quad (1)$$

where $i$ represents the number of each box; $n$ is the number of total boxes; $Ra^{i}_{avg}$ is the average radium activity measured in each box; $A_i$ is the area of each box; $A_{tot}$ is the total surface area of the system. In this study, the BB and WQ were divided into four and three boxes, respectively. The calculated area-weighted average radium activities were 25.40 dpm 100 L$^{-1}$ in the BB and 15.60 dpm 100 L$^{-1}$ in the WQ region.

### 3.2. Ra activities in the groundwater along the riverbank

The activities of $^{226}$Ra in the groundwater ranged from values lower than in the estuary to two values ten times higher than those found in the bay/estuary (Table 2). The radium activities in the wells near the mouth of the BB were lower than in the wells farther from the mouth. This was probably due to the different residence times of the well water, i.e., there was longer contact time between the well water and the minerals farther from the mouth. Near the mouth, the groundwater may rapidly discharge into the estuaries through tidal pumping. Because our samples all came from drinking water wells, the salinity of these fresh groundwater samples was low. The depths of most wells ranged from 2 to 5 m, suggesting they contained shallow groundwater from the surficial aquifer that was primarily recharged by rainfall infiltration. The groundwater $^{228}$Ra/$^{226}$Ra AR of 1.2 (n = 11), obtained from the linear regression line of the $^{228}$Ra vs. $^{226}$Ra plot of all of the groundwater samples, indicated a rather homogenous source, consistent with shallow seepage from the surficial aquifer.

## 4. Discussion

### 4.1. Sources of radium from various terms

The distribution of $^{226}$Ra relative to salinity (Fig. 2) displays non-conservative increases in the estuarine mixing zone in our study area. The sources of the extra Ra include desorption of Ra from river-borne particles and estuarine sediments, and submarine groundwater discharge. These source terms will be discussed and evaluated in the following section.

#### 4.1.1. Riverine

There are two contributors to this source: dissolved radium and desorbable radium. The riverine dissolved $^{226}$Ra activity was 24.0 dpm 100 L$^{-1}$ in the BB (average of stations BB1 and BB6) and 10.5 dpm 100 L$^{-1}$ in the WQ (average of stations WQ3, WQ16 and

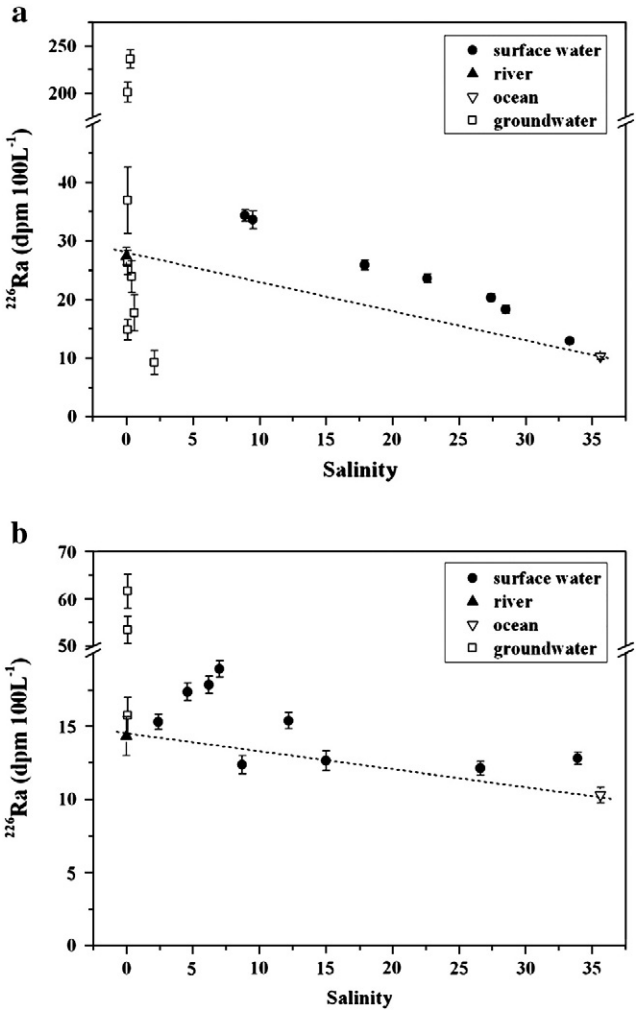


**Fig. 2.** Plots of dissolved $^{226}$Ra versus salinity for all the water samples collected in the Bamen Bay (a) and Wanquan River estuary (b) showing the mixing from river, ocean and groundwater end-members. The river end-member includes the dissolved and desorbed radium. The short dashed line represents the conservative mixing line between river and seawater end-members. Note the scale breaks on the y-axis of both plots.

WQ23). For desorbable radium, radium on the riverine suspended particles can be desorbed and added into the dissolved phase when these particles encounter seawater (Li et al., 1977; Krest et al., 1999). In this study, the desorbed activity of radium ($A_{river\text{-}des}$, dpm 100 L$^{-1}$) was estimated as:

$$A_{river-des} = (A^*_{sus} - A_{sed}) \cdot SPM^* \quad (2)$$

where $A^*_{sus}$ and $SPM^*$ represent the Ra activity on suspended particles and the suspended particle concentration in the river, respectively, and $A_{sed}$ is the average Ra activity on bottom sediments. Eq. (2) assumes that the suspended particles in the BB or WQ had the same exchange capacity as the surface sediments, i.e., the surface sediment activity was not diluted by coarse-grained materials. Table 3 shows all of the parameters used for the calculation of $A_{river\text{-}des}$ in the BB and WQ. Specifically, $A^*_{sus}$ and $A_{sed}$ of $^{226}$Ra in the BB region were 5.22 and 1.29 dpm g$^{-1}$, respectively. Thus, the maximum desorption of $^{226}$Ra would be 3.93 dpm g$^{-1}$. Combining this maximum desorption with the measured $SPM^*$ of 0.87 g 100 L$^{-1}$ resulted in a maximum desorption ($A_{river\text{-}des}$) of 3.42 dpm 100 L$^{-1}$ for $^{226}$Ra. The same calculation for the WQ region yielded the $A_{river\text{-}des}$ of 3.81 dpm 100 L$^{-1}$. The sum of dissolved and desorbed riverine inputs of $^{226}$Ra was 27.4 dpm 100 L$^{-1}$ in the BB and 14.3 dpm 100 L$^{-1}$ in the WQ, respectively. If conservative mixing only occurred between the river and seawater end-members from this point, the observed maximum $^{226}$Ra activity of 34.3 dpm 100 L$^{-1}$ in the BB and 18.3 dpm 100 L$^{-1}$ in the WQ would not be possible. Therefore, we need to find an additional source of Ra to maintain the balance of excess radium within the bay/estuary.

#### 4.1.2. Resuspension of bottom sediments and subsequent desorption of radium

Tidal currents and waves may resuspend sediments into the water column during estuarine mixing. Thus, the sediment-associated Ra, which comes from the production of desorbable Ra from the surface-bound Th parent, can be desorbed and added into the dissolved phase after the particles are resuspended (Krest et al., 1999; Beck et al., 2007). Beck et al. (2007) calculated the desorption fluxes of short-lived Ra isotopes ($^{224}$Ra and $^{223}$Ra) through this mechanism in Jamaica Bay; however, any release of long-lived $^{226}$Ra or $^{228}$Ra are negligible due to their long regeneration time. In our case, we made some appropriate changes to this reference for the calculation of $^{226}$Ra activity. The desorption activity of radium from resuspended sediments ($A_{sed\text{-}des}$, dpm 100 L$^{-1}$) is given by:

$$A_{sed-des} = (SPM_{ave} - SPM^*) \cdot A_{sed} \quad (3)$$

where $SPM_{ave}$ is the average suspended particle concentration in the bay/estuary. Here, we assume that (1) riverine particles comprise the major source for bottom sediments, (2) any increase in *SPM* is caused by sediment resuspension, and (3) up to 10% of the $^{226}$Ra on

**Table 2**
$^{226}$Ra and $^{228}$Ra activities (dpm 100 L$^{-1}$) and nutrient concentrations (μM) in groundwater samples collected around the Bamen Bay and Wanquan River estuary.

| Sample | Longitude (°E) | Latitude (°N) | Date (mm/dd/yy) | Salinity | $^{226}$Ra | Error | $^{228}$Ra | Error | DIN | DIP | DSi |
|---|---|---|---|---|---|---|---|---|---|---|---|
| Bamen Bay | | | | | | | | | | | |
| GW07 | 110.800 | 19.580 | 08/14/07 | 0.1 | 26.34 | 1.98 | 43.80 | 18.42 | 941 | 20.1 | 344 |
| GW12 | 110.800 | 19.555 | 08/16/07 | 0.1 | 14.88 | 1.74 | 57.54 | 3.48 | 348 | 0.16 | 305 |
| GW14 | 110.862 | 19.530 | 08/02/08 | 0.6 | 17.76 | 3.12 | 45.54 | 9.06 | 221 | 0.32 | 510 |
| GW15 | 110.942 | 19.610 | 08/02/08 | 0.4 | 23.94 | 2.70 | 33.60 | 6.00 | 1041 | 0.16 | 281 |
| GW20 | 110.805 | 19.628 | 08/04/08 | 0.1 | 201 | 10.50 | 236.6 | 15.36 | 252 | 0.24 | 318 |
| GW21 | 110.829 | 19.630 | 08/04/08 | 0.1 | 36.9 | 5.70 | 174.2 | 13.80 | 477 | 23.5 | 656 |
| GW22 | 110.892 | 19.626 | 08/04/08 | 0.3 | 235.9 | 9.54 | 360.2 | 14.82 | 834 | 0.63 | 619 |
| GW23 | 110.822 | 19.543 | 08/07/08 | 2.1 | 9.24 | 2.04 | 77.52 | 5.58 | 104 | 0.35 | 261 |
| Average | | | | | 70.75 | 92.0 | 128.6 | 118.4 | 527 | 5.68 | 412 |
| Wanquan River estuary | | | | | | | | | | | |
| GW03 | 110.556 | 19.137 | 08/13/07 | 0.1 | 15.72 | 1.26 | 25.26 | 3.6 | 1779 | 0.04 | 195 |
| GW04 | 110.586 | 19.162 | 08/13/07 | 0.1 | 53.4 | 2.88 | 109.1 | 17.94 | 1163 | 0.12 | 292 |
| GW10 | 110.520 | 19.058 | 08/15/07 | 0.1 | 61.56 | 3.54 | 87.0 | 4.56 | 828 | 6.99 | 589 |
| Average | | | | | 43.56 | 24.5 | 73.8 | 43.5 | 1257 | 2.38 | 359 |

**Table 3**
Desorption of $^{226}$Ra from both the riverine suspended particles and resuspension of bottom sediments in the Bamen Bay (BB) and Wanquan River estuary (WQ)[a].

| Panel A: Ra desorption from the riverine suspended particles | | | | |
|---|---|---|---|---|
| Region | $A^*_{sus}$ | $A_{sed}$ | SPM* | $A_{river\text{-}des}$ |
| BB | 5.22 | 1.29 | 0.87 | 3.42 |
| WQ | 6.11 | 1.29 | 0.79 | 3.81 |
| Panel B: Ra desorption from the resuspension of bottom sediments | | | | |
| Region | $SPM_{ave}$ | SPM* | $A_{sed}$ | $A_{sed\text{-}des}$ |
| BB | 6.2 | 0.87 | 1.29 | 0.69 |
| WQ | 5.1 | 0.79 | 1.29 | 0.56 |

[a] $A^*_{sus}$ and $A_{sed}$ units are dpm g$^{-1}$; $SPM_{ave}$ and $SPM^*$ are g 100 L$^{-1}$; $A_{river\text{-}des}$ and $A_{sed\text{-}des}$ are dpm 100 L$^{-1}$.

resuspended particles desorbs after resuspension (Gonneea et al., 2008). We calculated the initial Ra desorption event based on the difference between the Ra in the river SPM and the surface sediments. Because the river SPM loses almost all of its Ra upon entering the estuary (residual Ra trapped inside particles is not available for desorption), this approach should substantially overestimate Ra input from desorption. The $SPM_{ave}$ and $SPM^*$ in the BB were 6.2 and 0.87 g 100 L$^{-1}$,respectively, and thus the resuspension SPM was 5.3 g 100 L$^{-1}$. Combined with the $A_{sed}$ of 1.29 dpm g$^{-1}$ ($^{226}$Ra) and 10% desorption amount, the maximum desorption activity of $^{226}$Ra from the resuspended sediments into the water column was 0.69 dpm 100 L$^{-1}$ (Table 3). Similarly, $A_{sed\text{-}des}$ of 0.56 dpm 100 L$^{-1}$ ($^{226}$Ra) was obtained for the WQ. As expected, the contribution of Ra desorption from sediment resuspension was indeed insignificant compared with the riverine input.

#### 4.1.3. Diffusion of regenerated radium from sediment pore spaces

Another possible source of radium in the water column is a diffusive flux of radium through the sediment pore spaces. We follow the approach of Krest et al. (1999) to assess $^{226}$Ra supplied by diffusion and bioturbation from bottom sediments ($A_{sed\text{-}diff}$, dpm 100 L$^{-1}$).

$$A_{sed-diff} = F_{sed-diff} A_{surf} T / V \quad (4)$$

where $A_{surf}$ is the surface area of the study area (m$^2$), $T$ is the tidal period (ca. 0.75 days), and $V$ is the volume of the study area. We assume $F_{sed\text{-}diff} = 1.3 \times 10^{-5}$ dpm cm$^{-2}$ day$^{-1}$ (Krest et al., 1999). Using the parameters shown in Table 4, the estimated $A_{sed\text{-}diff}$ were 0.01 dpm 100 L$^{-1}$ in the BB and 0.004 dpm 100 L$^{-1}$ ($^{226}$Ra) in the WQ. It is clear that this source was negligible compared with the riverine input.

Because the Ra desorption from the riverine suspended particles is much more important than the desorption of Ra from the resuspended sediments and the diffusion of regenerated Ra from sediment pore spaces, we only consider the contribution from the river (dissolved and desorbed Ra) in the following section.

#### 4.1.4. Groundwater

As seen from the plots of $^{226}$Ra versus salinity for all of the water samples in the BB and WQ region, the majority of the data fall between the long-lived radium isotope composition of the river, seawater and groundwater end-members (Fig. 2). Fig. 3 shows the radium isotope composition for all of the groundwater samples in the BB and WQ regions. These BB data fall along a trend of $^{228}$Ra/$^{226}$Ra AR = 1.2; the WQ data have a slightly steeper slope, 1.6. Because these differences are small, we conclude that there was probably only one source of SGD coming from the surficial aquifer in each estuary. Most of the groundwater samples had $^{226}$Ra concentrations similar to the estuary samples; however, two samples in the BB were considerably enriched by a factor of 10. Clearly, the low activity groundwater samples could not enrich the estuary to the required concentration, so there must have been a significant contribution from the higher activity samples. Using the available data, it is difficult to evaluate the groundwater end-member concentration. We used the mean concentration from all samples in each region, with the caveat that the concentrations could be considerably higher. Although there are large uncertainties in the groundwater end-member concentration of SGD, using this averaged value allowed us to estimate a range of SGD fluxes to compare with other water sources in the bay/estuary.

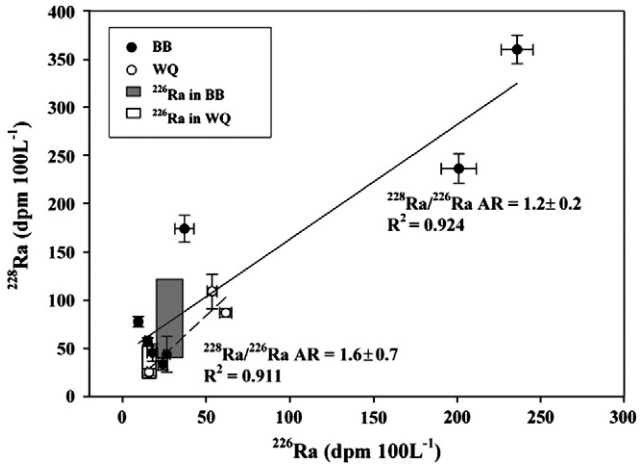


**Fig. 3.** $^{228}$Ra and $^{226}$Ra activities in all the groundwater samples collected around the Bamen Bay and Wanquan River estuary. The rectangle boxes show the ranges of $^{226}$Ra activities measured in surface waters in the BB and WQ, respectively.

### 4.2. Three-end-member mixing model of $^{226}$Ra balance

To resolve the relative end-member contributions to the BB and WQ systems, we followed the model of Moore (2003) and constructed a 3-end-member mixing model based on the water, radium ($^{226}$Ra), and salt balances to estimate the fractions of river, seawater and groundwater in the BB and WQ systems.

$$f_R + f_S + f_{GW} = 1.00 \quad (5)$$

$$^{226}Ra_R f_R + {}^{226}Ra_S f_S + {}^{226}Ra_{GW} f_{GW} = {}^{226}Ra_M \quad (6)$$

$$S_R f_R + S_S f_S + S_{GW} f_{GW} = S_M \quad (7)$$

where $f$ is the fraction of the river (R), seawater (S) and groundwater (GW) end-members; $^{226}Ra_R$ is $^{226}$Ra activity and $S_R$ is the salinity in the river end-member; $^{226}Ra_S$ is the $^{226}$Ra activity and $S_S$ is the salinity in the seawater end-member; $^{226}Ra_{GW}$ is the $^{226}$Ra activity and $S_{GW}$ is the salinity in the groundwater end-member; $^{226}Ra_M$ is the measured $^{226}$Ra activity and $S_M$ is the salinity measured in the water samples. These equations can be solved for the fractions of each end-member in each system.

We selected the following end-members in the BB to initialize the model: (1) the water sample at station BB12 represented the seawater end-member ($^{226}$Ra = 12.98 ± 0.44 dpm 100 L$^{-1}$ and salinity = 33.3),

**Table 4**
Diffusion of $^{226}$Ra from bottom sediments in the Bamen Bay (BB) and Wanquan River estuary (WQ)[a].

| Region | $F_{sed\text{-}diff}$ | $A_{surf}$ | V | $A_{sed\text{-}diff}$ |
|---|---|---|---|---|
| BB | 1.3 | 20 | 20 | 0.01 |
| WQ | 1.3 | 1.5 | 3.8 | 0.004 |

[a] $F_{sed\text{-}diff}$ unit is $10^{-5}$ dpm cm$^{-2}$ day$^{-1}$; $A_{surf}$ is $10^6$ m$^2$; $V$ is $10^6$ m$^3$; $A_{sed\text{-}diff}$ is dpm 100 L$^{-1}$.

(2) the river end-member included the dissolved and desorbed Ra ($^{226}$Ra = 27.38 ± 1.01 dpm 100 L$^{-1}$ and salinity = 0.0), and (3) the average activity of $^{226}$Ra in the groundwater samples around the BB represented the groundwater end-member ($^{226}$Ra = 70.75 ± 92.0 dpm 100 L$^{-1}$ and salinity = 0.48). Table 5 gives the results of this mixing model. For the WQ, the end-member values used for initializing Eqs. (5)–(7) and the corresponding results are summarized in Table 5 as well.

The fractions of each end-member were also normalized to area-weighted fractions to account for the heterogeneous distribution of the river, seawater and groundwater end-members. The area-weighted average fractions determined were $f_R = 0.27$, $f_S = 0.57$ and $f_{GW} = 0.16$ in the BB, and $f_R = 0.69$, $f_S = 0.24$ and $f_{GW} = 0.07$ in the WQ. The $f_R$ in the WQ was higher relative to that in the BB due to the larger discharge of the Wanquan River. However, the lower $f_{GW}$ in this region would contribute to the lower SGD rates. Had we used the higher groundwater concentrations of $^{226}$Ra in each system, the area-weighted average groundwater fractions would be reduced to about 0.03 in the BB and 0.04 in the WQ.

### 4.3. Flushing time

From the classical tidal prism method (Dyer and Taylor, 1973; Sanford et al., 1992), the average flushing time $T_f$ of a small and well-mixed embayment is defined as:

$$P = \int_H^0 A dz \tag{8}$$

$$T_f = \frac{VT}{(1-b)P} \tag{9}$$

where $P$ is the tidal prism, $A$ is the water surface area of the estuary, $z$ is the water depth over tidal range ($H$), $T$ is the tidal period, and $b$ is the return flow factor (a portion of the water that leaves the estuary during ebb tide and returns unmixed in the next flood tide). The volume of the estuary is defined as the product of the average area and depth. In the BB, because we do not know the water surface area between high and low tide, the tidal prism in Eq. (8) was determined by multiplying the average surface area by the tidal range during the sampling period. The parameters used for calculating the tidal prism are listed in Table 6.

Moore et al. (2006) used this model to calculate the flushing time in the Okatee River estuary. For the estimation of the return flow factor $b$, Moore et al. (2006) adopted two models: the physical model and the mixing model. In the mixing model, $b$ is estimated by sampling water returning to the estuary during rising tide. We assumed this water represents a mixture of the exported tidal prism and seawater. Thus, $b$ was simply the fraction of the seawater determined for the samples collected on the incoming tide, i.e., $f_S = b$. However, water samples with low salinity do not represent the tidal prism, so these were excluded from this calculation. The $b$ factor was estimated to be 0.78 (average of stations BB5, BB11 and BB14) in the BB and 0.78 (station WQ9) in the WQ. Using Eq. (9), the average flushing time in the BB and WQ were 3.9 ± 2.7 and 12.9 ± 9.3 days, respectively.

### 4.4. Submarine groundwater discharge (SGD) into the Bamen Bay and Wanquan River estuary

To quantify the submarine groundwater discharge (*SGD*, m$^3$ day$^{-1}$) into the BB and WQ, we must know the radium fluxes from the groundwater discharge ($F_{SGD}$, dpm day$^{-1}$) and the Ra end-member values for the potential groundwater seeping into the bay/estuary. $F_{SGD}$ equals the observed radium fluxes (*Flux*, dpm day$^{-1}$) within the system multiplied by the fractions of the groundwater end-member. *Flux* is obtained by dividing the radium inventory ($I$, dpm) by the flushing time ($T_f$, day). To calculate the inventory, we used the area-weighted average radium activities and volume in each system and assume that the water column is well mixed vertically (Liu et al., 2011). The inventories ($I$, dpm) of $^{226}$Ra were 5.1 × 10$^9$ dpm in the BB and 5.9 × 10$^8$ dpm in the WQ. Using the flushing times of 3.9 ± 2.7 and 12.9 ± 9.3 days in these systems, the $^{226}$Ra fluxes were 1.3 (±0.9) × 10$^9$ dpm day$^{-1}$ in the BB and 4.5 (±3.3) × 10$^7$ dpm day$^{-1}$ in the WQ.

The average $^{226}$Ra activities in the potential groundwater samples were 71 ± 92 dpm 100 L$^{-1}$ (n = 8) in the BB and 43.6 ± 24.5 dpm 100 L$^{-1}$ (n = 3) in the WQ. Meanwhile, the area-weighted average fractions of the groundwater end-members in the BB and WQ were 0.16 and 0.07, respectively. These data yield the SGD rates of 2.9 (±4.3) × 10$^5$ m$^3$ day$^{-1}$ (3.4 ± 5.0 m$^3$ s$^{-1}$) in the BB and 7.3 (±6.7) × 10$^3$ m$^3$ day$^{-1}$ (0.08 ± 0.08 m$^3$ s$^{-1}$) in the WQ. These contributions are ~16% and ~0.06% of the local surface water discharge; if we

**Table 5**
Results of the 3-end-member mixing model giving the fractions of river, seawater and groundwater end-members in each sample in the Bamen Bay and Wanquan River estuary.

| Station | Salinity | $^{226}$Ra (dpm 100 L$^{-1}$) | $f_R$ | $f_S$ | $f_{GW}$ |
|---|---|---|---|---|---|
| *Bamen Bay* | | | | | |
| End-member | | | | | |
| River[a] | 0.0 | 27.38 | | | |
| Seawater | 33.3 | 12.98 | | | |
| Groundwater | 0.48 | 70.75 | | | |
| *Surface water* | | | | | |
| BB3 | 17.9 | 25.94 | 0.32 | 0.54 | 0.14 |
| BB5 | 22.6 | 23.66 | 0.18 | 0.68 | 0.14 |
| BB7 | 9.5 | 33.60 | 0.48 | 0.28 | 0.24 |
| BB11 | 28.5 | 18.34 | 0.07 | 0.85 | 0.08 |
| BB14 | 27.4 | 20.38 | 0.07 | 0.82 | 0.11 |
| BB16 | 8.9 | 34.32 | 0.49 | 0.26 | 0.25 |
| Area-weighted averages | | | 0.27 | 0.57 | 0.16 |
| *Wanquan River estuary* | | | | | |
| End-member | | | | | |
| River[a] | 0.0 | 14.31 | | | |
| Seawater | 33.9 | 12.79 | | | |
| Groundwater | 0.1 | 43.56 | | | |
| *Surface water* | | | | | |
| WQ2 | 2.4 | 15.30 | 0.89 | 0.07 | 0.04 |
| WQ6 | 7.0 | 18.93 | 0.63 | 0.21 | 0.17 |
| WQ7 | 4.6 | 17.36 | 0.75 | 0.14 | 0.11 |
| WQ9 | 26.6 | 12.12 | 0.25 | 0.78 | −0.03 |
| WQ10 | 12.2 | 15.37 | 0.59 | 0.36 | 0.05 |
| WQ11 | 6.2 | 17.84 | 0.69 | 0.18 | 0.13 |
| WQ12 | 8.7 | 12.36 | 0.80 | 0.26 | −0.05 |
| WQ20 | 15.0 | 12.63 | 0.59 | 0.44 | −0.03 |
| Area-weighted averages | | | 0.69 | 0.24 | 0.07 |

[a] River end-member Ra = riverine dissolved Ra + riverine desorbed Ra.

**Table 6**
Summary of parameters used to calculate flushing time in the Bamen Bay and Wanquan River estuary.

| | Bamen Bay | Wanquan River estuary |
|---|---|---|
| Mean area, 10$^6$ m$^2$ | 20 | 1.5 |
| Tidal range, m | 0.88 ± 0.53 | 0.66 ± 0.42 |
| Prism, 10$^6$ m$^3$ | 17.6 ± 10.6 | 1.0 ± 0.63 |
| Mean depth, m | 1.0 | 2.5 |
| Mean volume, 10$^6$ m$^3$ | 20 | 3.75 |
| Tidal period, days | 0.75 ± 0.25 | 0.75 ± 0.25 |
| $b$ | 0.78 | 0.78 |
| $T_f$, days | 3.9 ± 2.7 | 12.9 ± 9.3 |

had used the highest $^{226}Ra$ activities in groundwater, the SGD rates would decrease by a factor of 18 to $0.19 \pm 0.13$ $m^3$ $s^{-1}$ in the BB and a factor of 3 to $0.03 \pm 0.02$ $m^3$ $s^{-1}$ in the WQ, or ~1% and ~0.03% of the local river discharge, respectively. In addition, the monitoring data in the BB system showed that domestic and industrial wastewater inflow into the bay were approximately 0.5 $m^3$ $s^{-1}$, and aquaculture effluents entering the bay were estimated at 6.7 $m^3$ $s^{-1}$ (Liu et al., 2011). Our SGD estimates were comparable with these values, which are considered to be an important part of the assessment of water budgets.

### 4.5. Evaluation of SGD-derived nutrient fluxes to the Bamen Bay and Wanquan River estuary

Nutrient transport through the coastal groundwater has been shown to be an important component of the nutrient budget in coastal water. Given the generally low velocities of groundwater, there is normally ample time for rock–water interactions in the aquifer, such as mineral dissolution reactions and surface processes (e.g., adsorption and desorption). The concentrations of some nutrients in coastal aquifers may be significantly elevated relative to river water and seawater (Moore et al., 2006). The nutrient inputs through the submarine groundwater discharge into the bay/estuary were determined by multiplying the SGD rates ($3.4 \pm 5.0$ $m^3$ $s^{-1}$ in the BB and $0.08 \pm 0.08$ $m^3$ $s^{-1}$ in the WQ) by the product of the nutrient concentrations in the groundwater. In this study, given that all of the groundwater samples were fresh and the well locations were several meters or kilometers from the discharge point, we assumed that no attenuation or chemical transformations of nutrients occur within the aquifer (or the subterranean estuary); such changes would alter our conclusions. The nutrient inputs through river water were determined by multiplying the river discharge (Wenchang River: 9.1 $m^3$ $s^{-1}$; Wenjiao River: 11.6 $m^3$ $s^{-1}$; Wanquan River: 136 $m^3$ $s^{-1}$) by the concentrations of the nutrients in river water (Wenchang River: 88.6, 0.63 and 164 μM; Wenjiao River: 81.5, 0.84 and 150 μM; Wanquan River: 50.9, 0.72 and 327 μM for DIN, DIP and DSi, respectively).

In our study, the average groundwater concentrations in the BB region were $527 \pm 361$, $6 \pm 10$ and $412 \pm 159$ μM (n = 8) for DIN, DIP and DSi, respectively (Table 2). The SGD-derived nutrient loads were $1.6 (\pm 2.5) \times 10^5$, $1.7 (\pm 3.8) \times 10^3$ and $1.2 (\pm 1.8) \times 10^5$ mol $day^{-1}$ for DIN, DIP and DSi, respectively (Table 7). A recent study by Liu et al. (2011) had estimated the dissolved nutrients loading to the BB region from conventional sources. When our results are compared with these nutrient mass balance components, such as river input (DIN = $1.3 (\pm 0.5) \times 10^5$, DIP = $1.2 (\pm 0.5) \times 10^3$, DSi = $2.5 (\pm 0.3) \times 10^5$ mol $day^{-1}$), atmospheric deposition (DIN = $4.2 (\pm 1.0) \times 10^3$, DIP = 27.4, DSi = $1.1 (\pm 0.3) \times 10^2$ mol $day^{-1}$), aquaculture effluents (DIN = $4.3 (\pm 7.6) \times 10^4$, DIP = $1.5 (\pm 2.2) \times 10^3$, DSi = $3.6 (\pm 3.0) \times 10^4$ mol $day^{-1}$) and wastewater discharge (DIN = $2.9 (\pm 0.8) \times 10^3$, DIP = 27.4, DSi = $7.9 (\pm 2.4) \times 10^3$ mol $day^{-1}$) (Liu et al., 2011), the role of SGD in the nutrient loading estimates to the BB becomes apparent; it contributed on the order of 50%, 31% and 34% of the total inputs for DIN, DIP and DSi, respectively, in the summer period. Thus, the nutrient inputs through SGD appeared to be the dominant source of DIN in this bay and to contribute to the overall nutrient status, even though the SGD rates may not rival river discharge in total volume.

Organic matter degradation and denitrification may take place in the summer, causing the removal or regeneration of dissolved nutrients and potentially causing the inputs from SGD to be smoothed out or masked (Liu et al., 2011). Nevertheless, we observed a general trend of increasing nutrient concentrations when salinity was below 10 and decreasing nutrient concentrations above this salinity. This was consistent with the salinity mixing curves that indicate that excess Ra input occurred only at the low salinity end of the bay.

For the WQ system, the average concentrations of nutrients in the groundwater were $1257 \pm 482$, $2.4 \pm 4$ and $359 \pm 205$ μM (n = 3) for DIN, DIP and DSi, respectively (Table 2). The SGD associated nutrient fluxes were 9.2 $(\pm 9.1) \times 10^3$, $17.5 \pm 33.2$ and 2.6 $(\pm 2.8) \times 10^3$ mol-$day^{-1}$ for DIN, DIP and DSi, respectively. For comparison, the nutrient inputs through the Wanquan River were $6.0 \times 10^5$, $8.5 \times 10^3$, $3.8 \times 10^6$ mol $day^{-1}$ for DIN, DIP and DSi, respectively (Table 7). Clearly, the nutrient fluxes from submarine groundwater discharge were lower than that from the local river input, comprising up to 3%, 0.6% and 0.1% of the river loading estimates (DIN, DIP and DSi, respectively). This indicates that the SGD-derived nutrient fluxes are not a major source of new nutrient input for this estuary.

Groundwater N:P ratios are commonly much higher than the requirements by phytoplankton growth (Redfield N:P ratio of 16:1) in that P in groundwater is more efficiently immobilized than N (Slomp and Van Cappellen, 2004). In our groundwater study, though the N:P ratios were greater than the Redfield ratio, they were not significantly different from the values found for the river water (Table 7). Because the number of our samples was limited, this estimate carried large uncertainties. This phenomenon has also been observed in other coastal regions. For example, the N:P ratios in groundwater were 660 around the southern Rhode Island (Kelly and Moran, 2002), 792 in the Yeongil Bay, Korea (Kim et al., 2008), and 78 in the Hampyeong Bay, Korea (Waska and Kim, 2011). High N:P ratios in groundwater discharge could affect the ecology of coastal waters by forcing the present N-limited coastal primary production towards P-limitation (Lapointe et al., 1990; Slomp and Van Cappellen, 2004). It has also been shown that the SGD-driven nutrients also have a significant effect on changing the microalgal community composition in coastal areas (Lee and Kim, 2007; Lee et al., 2010). This may, in turn, contribute to the occurrence of algal blooms as the outbreaks of algae are often accompanied by one of a group of fast-growing opportunistic algae that flourish when the environment is flushed by SGD, i. e., toxic diatom *Pseudo-nitzschia* spp. in Alabama coastal waters (Liefer et al., 2009), dinoflagellate red-tide outbreaks in the southern sea of Korea (Lee and Kim, 2007), brown-tide blooms in a Long Island embayment (Gobler and Sañudo-Wilhelmy, 2001), and harmful *Karenia brevis* blooms off Florida (Hu et al., 2006) (Lee et al., 2010).

We conclude that the submarine groundwater discharge with high N:P ratios may have a significant effect on the coastal ecosystems of the east Hainan Island by influencing the stoichiometry of the coastal ecosystem or community composition of phytoplankton; these effects should be further investigated in the future. Moreover, the supply of DIN, DIP and DSi to the studied area through SGD was a significant contributor to the overall nutrient budget in the summer, especially in the BB region.

**Table 7**
Summary of SGD-derived nutrient fluxes compared to those from local rivers ($10^4$ mol $day^{-1}$).

| Region | DIN | DIP | DIN:DIP | DSi |
|---|---|---|---|---|
| *SGD-derived fluxes* | | | | |
| Bamen Bay | $15.5 \pm 25.1$ | $0.17 \pm 0.38$ | $92 \pm 259$ | $12.1 \pm 18.4$ |
| Wanquan River estuary | $0.92 \pm 0.91$ | $0.002 \pm 0.003$ | $524 \pm 1123$ | $0.26 \pm 0.28$ |
| *Local river fluxes* | | | | |
| Wenchang River | $6.99 \pm 2.63$ | $0.049 \pm 0.03$ | $143 \pm 103$ | $12.9 \pm 0.9$ |
| Wenjiao River | $6.41 \pm 3.97$ | $0.066 \pm 0.038$ | $97 \pm 82$ | $11.8 \pm 2.7$ |
| Wanquan River | 60 | 0.85 | 71 | 384 |

## 5. Concluding remarks

Along the northeastern coastline of Hainan Island, China (with a mean annual precipitation of 1800–1900 mm), nutrient inputs from the shallow groundwater discharge into the coastal region can have significant impacts on the coastal ecosystems. From the distribution

patterns of the $^{226}$Ra tracer in the surface water, sediments and shallow groundwater, we draw the following conclusions:

1 Excess Ra inputs were found in two coastal systems, the Bamen Bay region and, to a lesser extent, the Wanquan River estuary. The radium sources from the river and sediments cannot balance the radium budgets; thus, another important source from groundwater discharge must be considered.
2 A comparison of the nutrient fluxes through the submarine groundwater discharge with the other nutrient mass balance components in the Bamen Bay region, i.e., local river, atmospheric deposition, aquaculture effluents and wastewater discharge, reveals that nutrient input to this coastal area via SGD was a potentially important source of nutrients and must be considered when assessing the nutrient budgets. In the Wanquan River estuary, the SGD-derived nutrient loading did not appear to be a major source of nutrient input. Nevertheless, the submarine discharge of nutrient-enriched groundwater with high N:P ratios may have an important impact on the coastal ecosystems of east Hainan by controlling the water quality in the adjacent sea by altering the stoichiometry of the N:P ratios. These effects should be further investigated.

## Acknowledgements

We would like to thank the associated editor and three anonymous reviewers for very constructive and detailed comments. This research was supported by the Natural Science Foundation of China (41021064, 40925017), 111 Project (B08022), opening fund of SKLEC, and the PhD Program Scholarship Fund of ECNU (2010047).

## References

Baskaran M, Murray DJ, Santschi PH, Orr JC, Schink DR. A method for rapid in situ extraction and laboratory determination of Th, Pb, and Ra isotopes from large volumes of seawater. Deep-Sea Res 1993;40:849–65.
Beck AJ, Rapaglia JP, Cochran JK, Bokuniewicz HJ. Radium mass-balance in Jamaica Bay, NY: evidence for a substantial flux of submarine groundwater. Mar Chem 2007;106:419–41.
Burnett WC, Aggarwal PK, Aureli A, Bokuniewicz H, Cable JE, Charette MA, et al. Quantifying submarine groundwater discharge in the coastal zone via multiple methods. Sci Total Environ 2006;367:498–543.
Burnett WC, Bokuniewicz H, Huettel M, Moore WS, Taniguchi M. Groundwater and pore water inputs to the coastal zone. Biogeochemistry 2003;66:3–33.
Burnett WC, Chanton J, Christoff J, Kontar E, Krupa S, Lambert M, et al. Assessing methodologies for measuring groundwater discharge to the ocean. EOS Trans Amer Geophys Union 2002;83(11):117–23.
Burnett WC, Cowart JB, Deetae S. Radium in the Suwannee River and estuary—spring and river input to the Gulf of Mexico. Biogeochemistry 1990;10:237–55.
Burnett WC, Dulaiova H. Estimating the dynamics of groundwater input into the coastal zone via continuous radon-222 measurements. J Environ Radioact 2003;69:21–35.
Burnett WC, Kim G, Lane-Smith D. A continuous radon monitor for assessment of radon in coastal ocean waters. J Radioanal Nucl Chem 2001;249:167–72.
Charette MA, Buesseler KO, Andrews JE. Utility of radium isotopes for evaluating the input and transport of groundwater-derived nitrogen to a Cape Cod estuary. Limnol Oceanogr 2001;46:465–70.
Ding SJ, Liao XJ, Feng YS, Xu ZS. Geological environment in northeastern Hainan Island. Beijing: Geology press; 2007. p. p66. in Chinese.
Dulaiova H, Burnett WC, Chanton JP, Moore WS, Bokuniewicz HJ, Charette MA, et al. Assessment of groundwater discharges into West Neck Bay, New York, via natural tracers. Cont Shelf Res 2006;26:1971–83.
Dyer KR, Taylor PA. A simple, segmented prism model of tidal mixing in well-mixed estuaries. Estuar Coast Mar Sci 1973;1:411–8.
Elsinger RJ, Moore WS. $^{226}$Ra behavior in the Pee Dee River–Winyah Bay estuary. Earth Planet Sci Lett 1980;48:239–49.
Garcia-Solsona E, Garcia-Orellana J, Masque P, Garces E, Radakovitch O, Mayer A. An assessment of karstic submarine groundwater and associated nutrient discharge to a Mediterranean coastal area (Balearic Islands, Spain) using radium isotopes. Biogeochemistry 2010;97:211–29.
Ge CD, Slaymaker O, Pedersen TF. Change in the sedimentary environment of Wanquan River Estuary, Hainan Island, China. Chin Sci Bull 2003;48(21):2357–61.
Gobler CJ, Sañudo-Wilhelmy SA. Temporal variability of groundwater seepage and brown tide blooms in a Long Island embayment. Mar Ecol Prog Ser 2001;217:299–309.
Gonneea ME, Morris PJ, Dulaiova H, Charette MA. New perspectives on radium behavior within a subterranean estuary. Mar Chem 2008;109:250–67.
Hancock GJ, Martin P. Determination of Ra in environmental samples by alpha-particle spectrometry. Appl Radiat Isot 1991;42:63–9.
Hu C, Muller-Karger FE, Swarzenski PW. Hurricanes, submarine groundwater discharge, and Florida's red tides. Geophys Res Lett 2006;33:L11601.1–5. doi:10.1029/2005GL025449.
Hussain N, Church TM, Kim G. Use of $^{222}$Rn and $^{226}$Ra to trace groundwater discharge into the Chesapeake Bay. Mar Chem 1999;65:127–34.
Kelly RP, Moran SB. Seasonal changes in groundwater input to a well-mixed estuary estimated using radium isotopes and implications for coastal nutrient budgets. Limnol Oceanogr 2002;47:1796–807.
Key RM, Stallard RF, Moore WS, Sarmiento JL. Distribution and flux of $^{226}$Ra and $^{228}$Ra in the Amazon River estuary. J Geophys Res 1985;90:6995–7004.
Kim G, Ryu JW, Hwang DW. Radium tracing of submarine groundwater discharge (SGD) and associated nutrient fluxes in a highly-permeable bed coastal zone, Korea. Mar Chem 2008;109:307–17.
Krest JM, Moore WS, Gardner LR, Morris J. Marsh nutrient export supplied by groundwater discharge: evidence from Ra measurements. Global Biogeochem Cycle 2000;14:167–76.
Krest JM, Moore WS, Rama. $^{226}$Ra and $^{228}$Ra in the mixing zones of the Mississippi and Atchafalaya Rivers: indicators of groundwater input. Mar Chem 1999;64:129–52.
Lapointe BE, O'Connell JD, Garrett GS. Nutrient couplings between on-site sewage disposal systems, groundwaters, and nearshore surface waters of the Florida Keys. Biogeochemistry 1990;10:289–307.
Lee DR. A device for measuring seepage flux in lakes and estuaries. Limnol Oceanogr 1977;22:140–7.
Lee YW, Kim G. Linking groundwater-borne nutrients and dinoflagellate red-tide outbreaks in the southern sea of Korea using a Ra tracer. Estuar Coast Shelf Sci 2007;71:309–17.
Lee YW, Kim G, Lim WA, Hwang DW. A relationship between submarine groundwater-borne nutrients traced by Ra isotopes and the intensity of dinoflagellate red-tides occurring in the southern Sea of Korea. Limnol. Oceanogr 2010;55(1):1–10.
Li YH, Mathieu G, Biscaye P, Simpson HJ. The flux of $^{226}$Ra from estuarine and continental shelf sediments. Earth Planet Sci Lett 1977;37:237–41.
Liefer JD, MacIntyre HL, Novoveska L, Smith WL, Dorsey CP. Temporal and spatial variability in *Pseudo-nitzschia* spp. in Alabama coastal waters: a "hot spot" linked to submarine groundwater discharge? Harmful Algae 2009;8:706–14.
Liu CH, Jay JA, Ford TE. Evaluation of environmental effects on metal transport from capped contaminated sediment under conditions of submarine groundwater discharge. Environ Sci Technol 2001;35:4549–55.
Liu SM, Hong GH, Zhang J, Ye XW, Jiang XL. Nutrient budgets for large Chinese estuaries. Biogeosciences 2009;6:2245–63.
Liu SM, Li RH, Zhang GL, Wang DR, Du JZ, Herbeck LS. The impact of anthropogenic activities on nutrient dynamics in the tropical Wenchanghe and Wenjiaohe estuary and lagoon system in East Hainan, China. Mar Chem 2011;125:49–68.
Liu SM, Zhang J, Chen HT, Zhang GS. Factors influencing nutrient dynamics in the eutrophic Jiaozhou Bay, North China. Prog Oceanogr 2005;66:66–85.
Mao LM, Zhang YL, Bi H. Modern pollen deposits in coastal mangrove swamps from northern Hainan Island, China. J Coast Res 2006;22(6):1423–36.
Michael HA, Lubetsky JS, Harvey CF. Characterizing submarine groundwater discharge: a seepage meter study in Waquoit Bay, Massachusetts. Geophys Res Lett 2003;30(6):30.1–4. doi:10.1029/2002GL016000.
Miller RL, Kraemer TF, Mcpherson BF. Radium and radon in Charlotte Harbor Estuary, Florida. Estuar Coast Shelf Sci 1990;31:439–57.
Moore WS. Sampling $^{228}$Ra in the deep ocean. Deep-Sea Res Oceanogr Abstr 1976;23:647–51.
Moore WS. Radium isotopes in the Chesapeake Bay. Estuar Coast Shelf Sci 1981;12: 713–23.
Moore WS. Large groundwater inputs to coastal waters revealed by $^{226}$Ra enrichments. Nature 1996;380:612–4.
Moore WS. The subterranean estuary: a reaction zone of groundwater and seawater. Mar Chem 1999;65:111–25.
Moore WS. Sources and fluxes of submarine groundwater discharge delineated by radium isotopes. Biogeochemistry 2003;66:75–93.
Moore WS. The effect of submarine groundwater discharge on the ocean. Annu Rev Mar Sci 2010;2:59–88.
Moore WS, Blanton JO, Joye SB. Estimates of flushing times, submarine groundwater discharge, and nutrient fluxes to Okatee Estuary, South Carolina. J Geophys Res 2006;111(C9):C09006.1–14. doi:10.1029/2005JC003041.
Moore WS, Krest J, Taylor G, Roggenstein E, Joye S, Lee R. Thermal evidence of water exchange through a coastal aquifer: implications for nutrient fluxes. Geophys Res Lett 2002;29(14):49.1–4. doi:10.1029/2002GL014923.
Paytan A, Shellenbarger GG, Street HJ, Gonneea EM, Davis K, Young BM, et al. Submarine groundwater discharge: an important source of new nutrients to coral reef ecosystems. Limnol Oceanogr 2005;51:343–8.
Rutgers van der Loeff MM, Moore WS. Determination of natural radioactive tracers. In: Grasshoff K, Ehrhardt M, Kremling K, editors. Methods of seawater analysis. 3rd ed. Verlag: Chemie, Weinheim; 1999. p. 365–97.. (Chapter 13).
Sanford LP, Boicourt WC, Rives SR. Model for estimating tidal flushing of small embayments. J Waterw Port C-ASCE 1992;118:635–54.
Slomp CP, Van Cappellen P. Nutrient inputs to the coastal ocean through submarine groundwater discharge: controls and potential impact. J Hydrology 2004;295: 64–86.
Swarzenski PW. U/Th series radionuclides as coastal groundwater tracers. Chem Rev 2007;107:663–74.
Swarzenski PW, Reich C, Kroeger KD, Baskaran M. Ra and Rn isotopes as natural tracers of submarine groundwater discharge in Tampa Bay, Florida. Mar Chem 2007;104:69–84.
Swarzenski PW, Reich CD, Spechler RM, Kindinger JL, Moore WS. Using multiple geochemical tracers to characterize the hydrogeology of the submarine spring off Crescent Beach, Florida. Chem Geol 2001;179:187–202.
Valiela I, Costa J, Foreman K, Teal JM, Howes B, Aubrey D. Transport of groundwater-borne nutrients from watersheds and their effects on coastal waters. Biogeochemistry 1990;10:177–97.

Wang BC, Chen SL, Gong WP, Ling WQ, Xu Y. Development and evolution of estuarine coast in Hainan Island. Beijing: Ocean Press; 2006 (in Chinese).
Wang Y. Features of Hainan Island coastal environment. Mar Geol Lett 2002;18(3):1–9. (in Chinese).
Waska H, Kim G. Submarine groundwater discharge (SGD) as a main nutrient source for benthic and water-column primary production in a large intertidal environment of the Yellow Sea. J Sea Res 2011;65:103–13.
Yang HS, Hwang DW, Kim G. Factors controlling excess radium in the Nakdong River estuary, Korea: submarine groundwater discharge versus desorption from riverine particles. Mar Chem 2002;78:1–8.
Zeng ZX, Zeng XZ. Physicogeography of the Hainan Island. Beijing: Science Press; 1989 (in Chinese).
Zhang L. Radium isotopes in Changjiang estuary and East China Sea and their application in analysis of mixing among multiple water masses [D]. Shanghai: East China Normal University; 2007. p. p.20.. (in Chinese).